

PCA-BASED DENOISING OF SENSOR PATTERN NOISE FOR SOURCE CAMERA IDENTIFICATION

Ruizhe Li, Yu Guan, and Chang-Tsun Li

Department of Computer Science, University of Warwick
Coventry, CV4 7AL, UK
ruizhe.li, g.yu, c-t.li@warwick.ac.uk

ABSTRACT

Sensor Pattern Noise (SPN) has been proved to be an inherent fingerprint of the imaging device for source identification. However, SPN extracted from digital images can be severely contaminated by scene details. Moreover, SPN with high dimensionality may cause excessive time cost on calculating correlation between SPNs, which will limit its applicability to the source camera identification or image classification with a large dataset. In this work, an effective scheme based on principal component analysis (PCA) is proposed to address these two problems. By transforming SPN into eigenspace spanned by the principal components, the scene details and trivial information can be significantly suppressed. In addition, due to the dimensionality reduction property of PCA, the size of SPN is greatly reduced, consequently reducing the time cost of calculating similarity between SPNs. Our experiments are conducted on the Dresden database, and results demonstrate that the proposed method outperforms could achieve the state-of-art performance in terms of the Receiver Operating Characteristic (ROC) curves while reducing the dimensionality of SPN.

Index Terms— Digital forensics, Source camera identification, image classification, Sensor pattern noise, Photo Response Non-Uniformity noise, PCA

1. INTRODUCTION

With the decreasing price of image acquisition device, digital images become more popular in our daily lives. At the meantime, the use of digital images in forensic investigations becomes more frequent and important. In some cases, forensic investigators need to identify the origin of images in order to link the images to a suspect. Therefore, effective techniques for identifying the origin of digital images are urgently needed.

Sensor pattern noises, extracted from digital images to serve as the unique fingerprints of imaging devices, have been proved as an effective way for digital camera identification. The deterministic component of SPN is primarily caused by

varying sensitivity of individual pixels to light due to the inhomogeneity of silicon wafers and imperfections introduced by the sensor manufacturing process. Because of the uniqueness of the inhomogeneity of silicon wafers and manufacturing imperfections, even sensors made from the same silicon wafer would possess uncorrelated SPNs, which makes SPN a robust fingerprint for identifying source devices.

There have been several studies focused on the SPN-based source camera identification in the recent years. Lukas *et al.* [1] first adopted a wavelet-based denoising technique to extract the sensor pattern noise as the link between the query image and its origin. Then, a sparse 3D transform-domain collaborative filtering is introduced by Dabov *et al.* [2] to extract the SPN. Since the main component in SPN is Photo Response Non-Uniformity noise (PRNU) which is a kind of multiplicative noise, Chen *et al.* [3] proposed a maximum likelihood method to estimate the corresponding multiplicative factor from the reference images. Later, Goljan *et al.* [4] introduced the Peak to Correlation Energy ratio (PCE) as a replacement for normalized correlation detector to reduce the false acceptance rate. In [5], Li pointed out that the noise residue contains significant characteristics of the SPN, but it can be easily contaminated by scene details. To address this issue, Li introduced an enhanced SPN by assigning higher weight to the reliable components. A further investigation into SPN's location-dependent quality is reported by Li and Satta in [6]. In [7], Li *et al.* proposed a Couple-Decoupled PRNU extraction method to prevent the CFA interpolation noise from propagating into the physical components. In [8], Wu *et al.* applied the context adaptive interpolation to predict the noise-free image for suppressing the impact of image content before SPN feature extraction.

There are two main challenging problems in the task of source camera identification. The first one, which most of prior works focused on, is that SPN can be easily contaminated by other noise components, such as image content, blocking artifacts introduced by JPEG compression, random noise, *etc.* As a result, the identification rate is unsatisfactory unless images of a large resolution are used. Secondly, in practice, analysts may need to decide whether a given image was taken by a camera whose SPN is in the database. Straightforward

calculating correlation between the query SPN and each reference SPN from the database has complexity proportional to the product of the database size and the dimensionality of SPN. SPN with high dimensionality therefore may cause excessive time cost in calculating correlations, which will limit its applicability to the source camera identification or image classification for a large sized database. In order to solve these problems, an effective method based on the principal component analysis is proposed in the work. Experimental results show that our method manage to suppress the impact of scene details while reducing the dimensionality of SPN.

The rest of this paper is organized as follows. In Section 2, we present the PCA-based denoising algorithm for the high dimensional SPN images. We also describe the way to estimate the reference feature for each camera in eigenspace as well as the detection statistic. Experimental results are reported in Section 3. Finally, conclusion is drawn in Section 4.

2. PROPOSED METHOD

PCA [9] is a decorrelation method which has been widely used for dimensionality reduction in pattern recognition and data compression. It also has been successfully employed for noise removal [10, 11]. In this work, we apply PCA to enhance the purity of SPN for the source camera identification purpose. The idea underlying our algorithm is that the energy of a signal will concentrate on a small subspace of the entire eigenspace, while the energy of noise will spread over the whole eigenspace. Therefore, by preserving only the most important subspace and then conducting the inverse PCA transform, the noise could be significantly attenuated while the signal being well recovered.

2.1. Training Set Construction

As we know that SPN is a subtle signal when compared to the contaminated noise introduced by image content. In order to avoid these noise components taking the dominant role in the eigenspace, we use SPN extracted from smooth images for PCA training, since there are no strong scene details in the smooth images. Such a training sample selection can better ensure that PCA is adopted to find the subspace which can best represent the SPN signal. We call this objective subspace as ‘‘SPN space’’ in the rest of this paper.

Assume there are n images $I_i (i = 1, 2, \dots, n)$ taken by c cameras and each camera has $L = n/c$ images. After cropping the center block $B_i \in \mathbb{R}^{N \times N}, i = 1, 2, \dots, n$ from the full-sized image, the Wiener filter is first used to extract the SPN W_i from B_i in the discrete wavelet domain, such that

$$W_i = DWT(B_i) - F(DWT(B_i)) \quad (1)$$

where $DWT(\cdot)$ is discrete wavelet transform and $F(\cdot)$ is the Wiener filter. Then the obtained W_i is transformed to the

spatial domain and reshaped to a column vector $\mathbf{x}_i \in \mathbb{R}^{N^2 \times 1}$. These n SPN images are used as the training set to construct the eigenspace.

2.2. PCA Denoising

Let $\Psi = \frac{1}{n} \sum_{i=1}^n \mathbf{x}_i$ be the mean of the training set. Each \mathbf{x}_i differs from the mean Ψ by the vector $\Phi_i = \mathbf{x}_i - \Psi$. Then PCA is performed to seek a set of orthonormal vectors \mathbf{u}_k and their associated eigenvalues λ_k . The vectors \mathbf{u}_k and scalars λ_k are the eigenvectors and eigenvalues, respectively, of the covariance matrix C

$$C = \frac{1}{n} \sum_{i=1}^n \Phi_i \Phi_i^T = \frac{1}{n} A A^T \quad (2)$$

where $A = [\Phi_1, \Phi_2, \dots, \Phi_n]$. However, when the size of image blocks is very large (e.g., $N \times N = 512 \times 512$ pixels), directly calculating eigenvectors of the large matrix $C \in \mathbb{R}^{N^2 \times N^2}$ is computationally prohibitive (with a time complexity $O(N^6)$). To make PCA feasible for large image blocks, we can apply a fast method instead to generate these eigenvectors (when $n \ll N^2$).

Assume \mathbf{u}_k' are the unit eigenvectors of $A^T A \in \mathbb{R}^{n \times n}$ with eigenvalue λ_k' . Therefore, we can obtain $A^T A \mathbf{u}_k' = \lambda_k' \mathbf{u}_k'$. Premultiplying both sides by A , then we have $A A^T (A \mathbf{u}_k') = \lambda_k' (A \mathbf{u}_k')$, where $A \mathbf{u}_k'$ are the eigenvectors of $A A^T = C$ with eigenvalues λ_k' . Thus, instead of finding the eigenvectors \mathbf{u}_k of matrix C directly, we calculate the eigenvectors \mathbf{u}_k' of the smaller matrix $A^T A \in \mathbb{R}^{n \times n}$ and obtain $\mathbf{u}_k = A \mathbf{u}_k'$. \mathbf{u}_k are then normalized to the unit vectors. In practise, the training set will be relatively small ($n \ll N^2$). Therefore, with this method, the time complexity can be reduced to $O(n^3)$.

By using this fast method, the entire eigenspace $M = [\mathbf{u}_1, \dots, \mathbf{u}_n]^T$ can be obtained. The eigenvectors with the d largest eigenvalues are then selected to construct the objective SPN space $M_{SPN} = [\mathbf{u}_1, \dots, \mathbf{u}_d]^T$. In this work, we keep the top d eigenvectors corresponding to 99% of the variance. For a given SPN \mathbf{x} , we can project it into the SPN space by a simple operation

$$\mathbf{y} = M_{SPN} \mathbf{x} \quad (3)$$

where \mathbf{y} is a new representation for SPN \mathbf{x} in the SPN space.

2.3. SPN Reconstruction

According to the obtained feature \mathbf{y} and SPN space M_{SPN} , it is easy to reconstruct SPN as follow

$$\mathbf{x}' = M_{SPN}^T \mathbf{y} \quad (4)$$

where \mathbf{x}' is an approximation for \mathbf{x} (when $d < n$). In particular, when the selected number of eigenvectors $d = n$, we have $\mathbf{x}' = \mathbf{x}$, which means the given SPN is completely reconstructed without any loss of information.

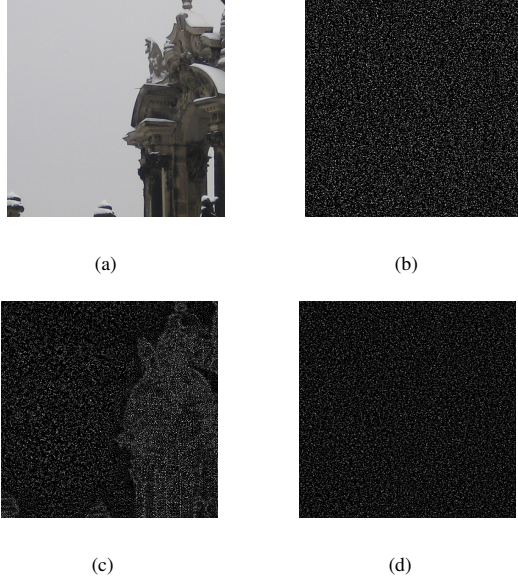


Fig. 1: (a) An image taken by Canon Ixus70. (b) Clean reference SPN. (c) The SPN extracted from (a) by the method mentioned in section 2.1. (d) The SPN reconstructed from (a) by the proposed method. (Note the intensity of Fig. 1(b), (c) and (d) has been scaled to the interval [0,255] for visualization purpose.)

By preserving only the d principal components and conducting the reconstruction, our method can significantly suppress the impact of image content. For example, Fig. 1(a)~(d) show a natural image taken by Canon Ixus70, the reference SPN of Canon Ixus70 (average SPN of 50 smooth and bright images taken by Canon Ixus70), the SPN extracted from the image of Fig. 1(a), and the reconstructed SPN, respectively. Fig. 2(b) is what a “clean” SPN should look like. From Fig. 1(c), we can see that the scene details in Fig. 1(a) propagate through the Wiener filter into the obtained SPN. However, these influential scene details have been significantly removed from our reconstructed SPN (see Fig. 1(d)). In this work, we use the feature \mathbf{y} in the flowing detection phase rather than the reconstructed SPN \mathbf{x}' , since feature \mathbf{y} has less dimensionality and the results of these two manners are almost the same.

2.4. Reference Estimation and Detection Statistics

We obtain the reference feature \mathbf{y}' for each camera by averaging all the feature vectors $\mathbf{y}_t (t = 1, \dots, L)$ estimated from images taken by that camera

$$\mathbf{y}' = \frac{\sum_{t=1}^L \mathbf{y}_t}{L} \quad (5)$$

where \mathbf{y}' is the reference feature for this camera.

The normalized cross-correlation (NCC) is used as the detection statistics to measure the similarity between the query

Table 1: Cameras used in our experiment

Cameras	Alias	Resolution
Samsung_NV15	C11	3648 × 2736
Canon_Ixus70_A	C21	3072 × 2304
Canon_Ixus70_B	C22	
Canon_Ixus70_C	C23	
Rollei_RCP_7325XS	C31	3072 × 2304
Samsung_L74wide_A	C41	3072 × 2304
Samsung_L74wide_B	C42	
Samsung_L74wide_C	C43	
Nikon_CoolPixS710_A	C51	4352 × 3264
Olympus_Mju_1050SW	C61	3648 × 2736

\mathbf{y} and the reference \mathbf{y}'

$$corr(\mathbf{y}, \mathbf{y}') = \frac{(\mathbf{y} - \bar{\mathbf{y}})(\mathbf{y}' - \bar{\mathbf{y}}')}{\|\mathbf{y} - \bar{\mathbf{y}}\| \|\mathbf{y}' - \bar{\mathbf{y}}'\|} \quad (6)$$

where $\bar{\mathbf{y}}$ and $\bar{\mathbf{y}}'$ are the means of \mathbf{y} and \mathbf{y}' , respectively. Notice that the size of feature vector $\mathbf{y} \in \mathbb{R}^{d \times 1}$ is much smaller than the size of SPN data $\mathbf{x} \in \mathbb{R}^{N^2 \times 1}$. It allows our method be more computationally effective in the detection phase than other existing methods.

3. EXPERIMENTS

3.1. Experiment Setting

In this section, the proposed method and some state-of-the-art schemes [1, 5, 8] are tested on the Dresden Image database [12]. A total of 2000 images from 10 cameras are involved in our experiments, each responsible for 200. These 10 camera devices belong to 6 camera models, each camera model has 1 or 3 different devices. These cameras are listed in Table 1. For each camera device, we have two sub-image datasets which are the reference image dataset (50 images) and test image dataset (150 images), respectively. Images in reference image dataset are the smooth and bright images and the test images are the natural scene pictures in daily life.

3.2. Performance Evaluation

The corresponding experimental results in terms of the Receiver Operating Characteristic are then used for presenting the accuracy of these four methods. For each chosen camera, we first estimate reference feature using $L = 50$ images from the reference image dataset. Then, 150 test images of this camera are selected as the intraclass samples and 1350 test images of the other 9 cameras (each responsible for 150) are selected as the interclass samples. Totally we get 150×10 intraclass and 1350×10 interclass samples of correlation values for the overall 10 cameras. To get the convincing results, all the 150×10 intraclass and 1350×10 interclass

samples from 10 cameras are used together to draw the overall ROC curve [1]. Instead of using the full size photo, both reference and test images are of three different sizes (*i.e.*, 128×128 , 256×256 and 512×512 pixels) cropped from the center of entire image. We extract SPNs from Red, Green and Blue channel separately and combine them by using the linear combination as in RGB to grayscale conversion. The experimental results as well as comparison with other methods are shown in Fig. 2~4.

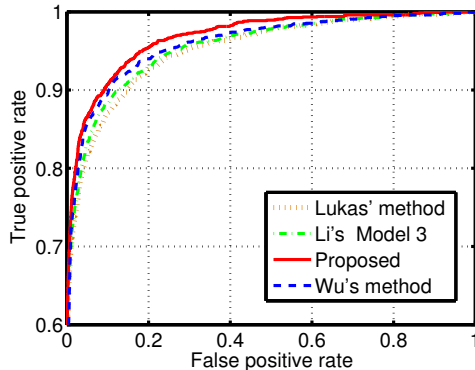


Fig. 2: The overall ROC curves on images with size of 128×128 pixels.

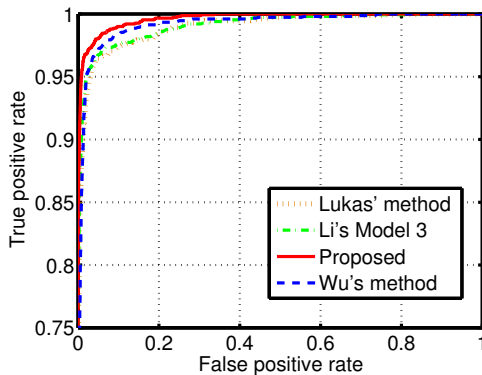


Fig. 3: The overall ROC curves on images with size of 256×256 pixels.

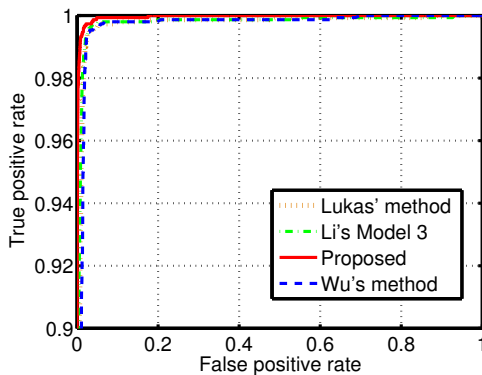


Fig. 4: The overall ROC curves on images with size of 512×512 pixels.

Table 2: Computational time of NCC for different methods on images with size of $N \times N$ pixels.

Methods	Detection Time (ms)		
	N=128	N=256	N=512
Proposed	0.05	0.05	0.05
Lukas'	0.40	1.64	6.60
Model 3	0.39	1.63	6.58
Wu's	0.39	1.64	6.59

The results show that the existing methods [1, 5, 8] can achieve nearly perfect experimental results on image blocks with large size (*i.e.*, 512×512 pixels). However, their performance on the small image blocks (*i.e.* 128×128 and 256×256 pixels) are still unsatisfactory. It is because small blocks tend to contain less SPN components, and are more easily polluted by the image content. All the three figures indicates that the proposed method outperforms other three methods [1, 5, 8], especially when images with small sizes. It means that our method is more effective on attenuating the effect of image content.

Table 2 presents the time cost of calculating NCC for four different methods. All the experimental works are conducted on the same PC with Intel(R) Core(TM) i5-3470 CPU @3.20GHz 16G RAM. The computational complexity of NCC depends on the dimensionality of the two participant features. In this experiment, the dimensionality of our feature is only $d \approx 200$ which is much smaller than that of the other methods N^2 ($d \ll N^2$). Therefore, the time cost of calculating NCC using the features obtained by the proposed method is only approximately 12.5%, 3.0% and 0.7% of that of the other three methods when $N=128$, $N=256$ and $N=512$ respectively. Moreover, the dimensionality of features obtained by Lukas' method, Li's model 3 and Wu's method are equal to image size (N^2). Therefore, as shown in Table 2 that the time cost of these three methods are almost the same at each image size, and that will significantly increase when image size is increasing. However, the dimensionality of our feature does not depend on the resolution of image but the number of training samples. Therefore, with increasing resolution of image, the proposed method always keeps at a constant low level even when image resolution is prohibitively large. Based on these observations, when compare to the time consumption of NCC of Lukas' method, Li's model 3 and Wu's method, it is easy to conclude that the larger image size is used, the more efficient the proposed method could be. And this improvement becomes more prominent when the number of query image is increasing.

4. CONCLUSION

In the past few years, researchers have made great efforts to improve the performance of the SPN-based source cam-

era identification. However, they lack considerations on the problem caused by the high dimensionality of SPN. High dimensional features inevitably aggravate the time spending on the detection phase, which degrades the identification performance. In this paper, we present a PCA-based SPN denoising scheme for source camera identification. To our best knowledge, such an approach has never been attempted in the area of SPN-based source device identification. There are two main advantages of the proposed method. First, due to the merit of dimensionality reduction of PCA, the proposed method can obtain a sparse representation with much lower dimensionality. Secondly, the proposed method manage to suppress the effect of scene details and improve the ROC performance of source camera identification. Experimental results have shown that our method could achieve the state-of-art ROC performance while reducing the dimensionality of SPN.

5. REFERENCES

- [1] J. Lukas, J. Fridrich, and M. Goljan, "Digital camera identification from sensor pattern noise," *IEEE Transactions on Information Forensics and Security*, vol. 1, no. 2, pp. 205–214, 2006.
- [2] K. Dabov, A. Foi, V. Katkovnik, and K. Egiazarian, "Image denoising by sparse 3d transform-domain collaborative filtering," *IEEE Transactions on Image Processing*, vol. 16, no. 8, pp. 2080–2095, 2007.
- [3] M. Chen, J. Fridrich, M. Goljan, and J. Lukas, "Determining image origin and integrity using sensor noise," *IEEE Transactions on Information Forensics and Security*, vol. 3, no. 1, pp. 74–90, 2008.
- [4] M. Goljan, "Digital camera identification from images - estimating false acceptance probability," in *Proc. of International Workshop on Digital-forensics and Watermarking*, pp. 454–468. 2009.
- [5] C.-T. Li, "Source camera identification using enhanced sensor pattern noise," *IEEE Transactions on Information Forensics and Security*, vol. 5, no. 2, pp. 280–287, 2010.
- [6] C.-T. Li and R. Satta, "Empirical investigation into the correlation between vignetting effect and the quality of sensor pattern noise," *IET Computer Vision*, vol. 6, no. 6, pp. 560–566, 2012.
- [7] C.-T. Li and Y. Li, "Color-decoupled photo response non-uniformity for digital image forensics," *IEEE Transactions on Circuits and Systems for Video Technology*, vol. 22, no. 2, pp. 260–271, 2012.
- [8] G. Wu, X. Kang, and K.J.R. Liu, "A context adaptive predictor of sensor pattern noise for camera source identification," in *Proc. of the IEEE International Conference on Image Processing*, pp. 237–240, 2012.
- [9] K. Fukunaga, *Introduction to Statistical Pattern Recognition*, 2nd ed. New York: Academic, 1991.
- [10] D. Zhang, R. Lukac, Xiaolin Wu, and D. Zhang, "Pca-based spatially adaptive denoising of cfa images for single-sensor digital cameras," *IEEE Transactions on Image Processing*, vol. 18, no. 4, pp. 797–812, 2009.
- [11] D.D. Muresan and T.W. Parks, "Adaptive principal components and image denoising," vol. 1, pp. I101–I104, 2003.
- [12] T. Gloe and R. Böhme, "The dresden image database for benchmarking digital image forensics," *Journal of Digital Forensic Practice*, vol. 3, no. 2-4, pp. 150–159, 2010.